Wave Length Shifter Strips and G-APD Arrays for the Read-Out of the z-Coordinate in Axial PET Modules

A. Braem, E. Chesi, C. Joram, A. Rudge, J. Séguinot, P. Weilhammer, R. De Leo, E. Nappi, W. Lustermann, D. Schinzel, I. Johnson, D. Renker and S. Albrecht

***Abstract*– The measurements presented in this paper are related to the development of a PET camera based on a 3D axial geometry with excellent 3-dimensional spatial, timing and energy resolution. The detector modules under development consist of matrices of long axially oriented scintillation crystal bars, which are individually coupled to photodetectors. The axial coordinate is derived from Wave Length Shifting (WLS) plastic strips orthogonally interleaved between the crystal bars and readout by G-APD arrays. We report on results from measurements with two LYSO crystal bars, read with PMTs, and two WLS strips readout with G-APD devices from Hamamatsu (called MPPC). The WLS strips are positioned orthogonally underneath the LYSO bars. Yields of about 80 photoelectrons from the WLS strips for an energy deposition in the LYSO crystals equivalent to the absorption of 511 keV photons are observed. The axial coordinate in the LYSO bars is reconstructed with a precision of about 1.9 mm (FWHM) using a digital reconstruction method. This resolution is still compromised by the availability of only two WLS strips and will improve with a full stack of LYSO crystals interleaved with WLS strip arrays, which is presently under development for a PET demonstrator set-up.**

I. INTRODUCTION

THE concept of a brain PET scanner module with axially arranged scintillation crystals has been described in detail in a previous publication [1]. This approach offers substantial advantages in performance compared with existing instruments. The main improvements in the new concept are true 3-D coordinate reconstruction of the 511 keV photon interaction and therefore no depth-of-interaction (DOI) uncertainty, spatial resolution depending only on the choice of the dimensions of the scintillator bars and WLS strips, high detection efficiency, uniformity of spatial resolution over the complete field of view, and capability to identify photon interactions with Compton cascades.

Manuscript received November 16, 2007.

A. Braem, E. Chesi, C. Joram, A. Rudge, J. Séguinot and P. Weilhammer are with CERN, PH Department, CH-1211 Geneva, Switzerland. P. Weilhammer is also affiliated to University / INFN Perugia, I-06100 Perugia, Italy.

R. De Leo and E. Nappi are with INFN, Sezione di Bari, I-70122 Bari, Italy.

W. Lustermann and D. Schinzel are with ETH Zürich, CH-8092 Zürich, Switzerland.

I. Johnson and D. Renker are with Paul Scherrer Institut, CH-5232 Villigen, Switzerland

S. Albrecht is with the University Hospital Geneva, CH-1211 Geneva, Switzerland

In a recent article [2] we demonstrated the potential of WLS strips to readout the axial z coordinate of a gamma interacting in long LYSO crystal bars ($3.2 \times 3.2 \times 100$ mm^3). However, in this work the strips were read out with conventional PMTs which would make it very difficult to realize large matrices of close crystal bars because of packaging constraints.

In this article we describe and discuss measurements using instead G-APD arrays to read out the WLS-strips. Thanks to their immunity to magnetic fields, the use of G-APDs for the readout of both crystals and WLS strips opens up the possibility of simultaneous co-registration of the PET data with MRI.

The G-APDs have a quantum efficiency QE of~ 30%, about twice the *QE* of PMTs at 490 nm wavelength, the emission peak of green WLS, which allows to obtain high detection efficiency, even for low energy recoil electrons from Compton interactions. Moreover, because of their size and geometric detection efficiency, G-APD arrays match the limited available space imposed by the design of matrices with closely stacked scintillating crystal bars [1].

II. EXPERIMENTAL PRINCIPLE AND SET-UP

In order to vary the energy deposition and its position along the LYSO crystal bars in an easily-controllable way, we used a pulsed and narrow low energy electron beam (Fig. 1) which impinges at normal incidence the surface of the crystal. The electrons are generated by illuminating a semi-transparent CsI photocathode of 10 nm thickness, vacuum deposited on a gold mesh (optical transparency $T \sim 0.90$) printed on a CaF_2 crystal disk, with short (~10 ns) UV light pulses. The light source, a self triggered H_2 flash lamp ($\lambda_{peak} = 160$ nm), is collimated in such a way that the light spot at the level of the photocathode has a Gaussian shape of 1.8 mm FWHM in both transversal coordinates (x, z).

A negative potential ($10 \text{ kV} \leq U_{acc} \leq 30 \text{ kV}$) is applied between the gold mesh underneath the CsI photocathode and a metallic transparent mesh ($T > 0.95$) at ground potential, mounted 0.5 mm above the LYSO bars. This configuration ensures a uniform parallel electric field which defines the kinetic energy of the accelerated electrons when they hit the crystals. Apart from the transverse point spread (~0.3 mm) the electron beam spot size is preserved from the photocathode to impact plane.

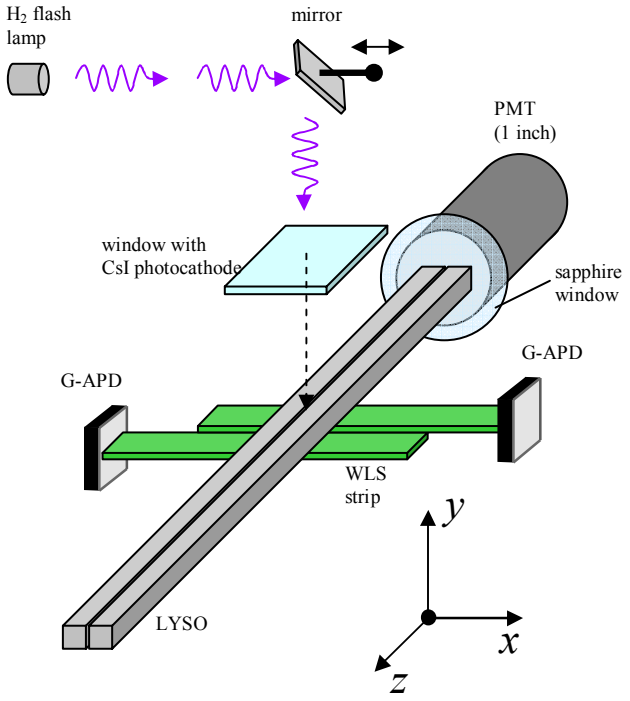

Fig. 1: Concept and schematic representation of the set-up.

The set-up allows (1) a precise adjustment of the energy deposited by controlling the number of photoelectrons N_{pe} emitted from the photocathode and the acceleration voltage U_{acc}, and (2) the scanning of the crystal surface by accurately displacing the light spot by means of a mirror indicated in Fig. 1.

The low energy range is of particular interest for the 3-D axial camera concept in order to unambiguously discriminate and precisely reconstruct Compton interactions in LYSO crystal matrices.

The measurements were performed in vacuum at a pressure of a few 10^{-6} mbar.

The test set-up comprises two closed optically polished LYSO:Ce crystals[1] (3.2 x 3.2 x 100 mm^3) mounted side by side with one of their end faces optically coupled through a vacuum tight thin (1 mm) sapphire window to a single PMT[2] . The opposite end faces of the bars are mirror coated with a vacuum evaporated Al film.

Two 60 mm long WLS strips[3] of 3 x 1.1 mm^2 cross section were mounted orthogonal and underneath the two LYSO crystals with a small gap. Each WLS strip was readout at opposite sides by a G-APD array from Hamamatsu[4] (MPPC[5] type S 10362-33-050 C) with 3 x 3 mm^2 active area. The strip end opposite to the MPPC was coated with a reflective Al film. Moreover, a thin Al foil underneath the WLS-strips reflects the small fraction of the non absorbed light back onto the strips increasing the total light path in the WLS strip, hence the absorption probability.

[1] Saint-Gobain Crystals, Nemours, France
[2] XP3102, Photonis. Brive-La Gaillarde, France.
[3] EJ-280-10x , ELJEN Technology, Sweetwater, Texas U.S.A.
[4] Hamamatsu Photonics K.K., Hamamatsu City, Japan.
[5] MPPC = Multi Pixel Photon Counter

III. Characterization of the Components

A. Physical properties and characterization of the WLS strips

The absorption peak of the ELJEN WLS plastic EJ-280 is centered at 425 nm, wavelength of the scintillation emission peak of LYSO crystals. The density of the plastic material is 1.02 g/cm^3 and its refractive index is 1.58. The fluorescent light of the plastic is shifted into the green range with a peak emission at 490 nm. The quantum efficiency of the fluorescent dye is 0.86 and its decay time 8.5 ns according to the specifications of the manufacturer.

For our application, on request, ELJEN produced WLS sheets (10 ×10 cm^2) of three different thickness (d_{strip} = 0.7, 1.1, 1.5 mm) with a dye concentration 10 times higher than their standard material in order to enhance the light absorption coefficient.

As illustration, Fig. 2 shows a measurement of the transmission coefficient versus the wavelength, performed with a spectrophotometer, for the three plastic sheet thicknesses. At 425 nm the three measurements are compatible with an absorption coefficient of 2.5 mm^{-1}. By using a reflector below the WLS strips as described above, more than 80% of the light entering the 0.7 mm thick strip can be absorbed.

WLS strips of 3 × 60 × d_{strip} mm^3 were produced by cutting the plastic sheets with a diamond saw and polishing the machined surfaces to a standard optical quality. In Fig. 3 the relative light yield is shown as a function of the distance to the readout PMT using a blue LED light source to excite the WLS material.

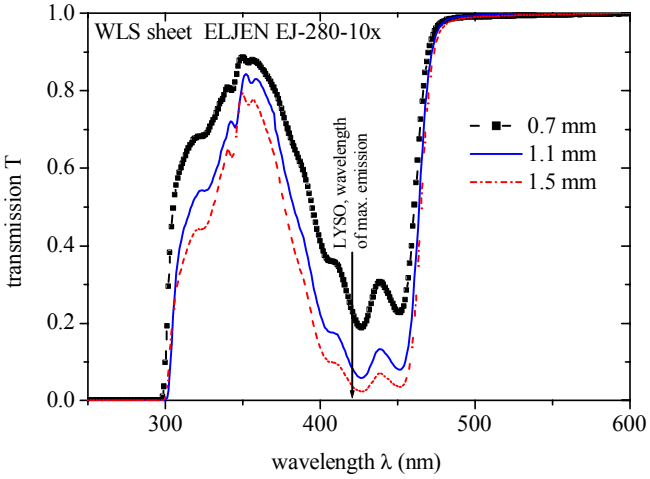

Fig. 2: Measured transmission coefficient for three sheets of high concentration WLS materials (0.7 mm, 1.1 mm and 1.5 mm thick). The data is corrected for the Fresnel reflections at the sheet/air interfaces. The corresponding absorption coefficient in the wavelength band 400 – 460 nm is around 2.5 mm^{-1}.

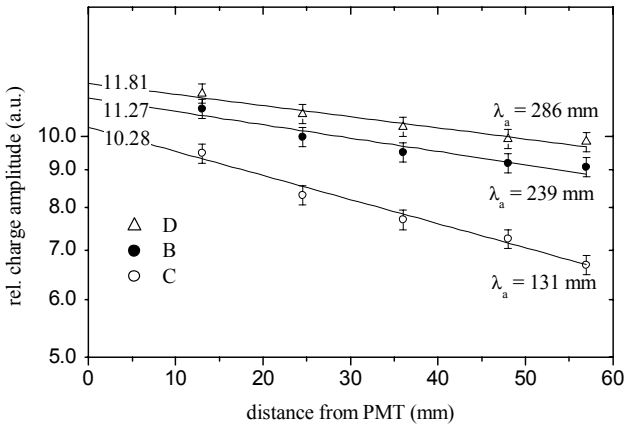

Fig. 3: Light absorption in WLS strips of 0.7 mm (C), 1.1 mm (B) and 1.5 mm (D) thickness. The plot shows the relative light output measured with a PMT at z = 0 as a function of the distance from the emission point. The data is fitted with exponentials yielding the absorption lengths λ_a = 131 mm, 239 mm and 287 mm.

B. *Characterization of the MPPC*

The MPPCs from Hamamatsu, type S 10362-33-050 C, are Geiger-APD arrays comprising 3600 pixels of 50 x 50 μm^2 covering a total area 3 x 3 mm^2 with a geometric efficiency of 61.5%. Following the specifications of the manufacturer the QE is about 35% at 400 nm for an avalanche gain of $5.7 \cdot 10^5$. This value includes the optical cross talk and the after pulses contributions.

Prior to the tests we have measured the performance of the MPPCs in the conditions of their use, i.e with a coupling to a fast voltage amplifier. The signals from the MPPCs were amplified by a factor 30, for matching to the readout electronics, with a fast voltage amplifier (ΔB = 150 Mhz, 50 ohm input impedance, 600 μV output noise) located inside the vacuum enclosure. These measurements performed by using a pulsed blue LED as light source are essential to correctly estimate the photoelectron yield of the WLS strips.

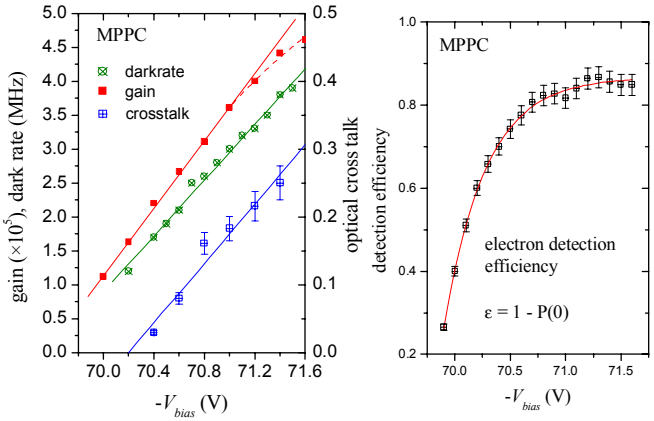

Fig. 4: Properties of the Hamamatsu MPPC 33-050C. Left hand side: Charge gain, dark count rate and optical cross-talk are plotted as function of the applied bias voltage. Right hand side: The detection efficiency □ for ≥1 photoelectron, obtained from the 'zero' count rate, is plotted versus the bias voltage.

Fig. 4 shows the results obtained at a temperature of 26°C for one of the MPPCs. Apart from an offset in the operating voltage both devices used show very similar characteristics. Fig. 4, left hand side, displays the variations of the gain with the applied voltage, the dark rate and the optical cross talk effect. Fig. 4, right hand side, shows the efficiency to detect one ore more photoelectrons as a function of the bias voltage. The efficiency ε is derived from the Poisson probability $P(0)$ to measure 0 photoelectrons while on average μ photoelectrons are detected: $\varepsilon = 1\text{-}P(0) = 1\text{-}e^{-\mu}$.

C. *Electron beam energy :*

For a relatively small number of electrons (< 30) the fluctuation $\sigma(N_e) = \sqrt{N_e}$ dominates the charge distribution measured at the output of the LYSO/PMT over the photoelectron statistic of the detected scintillation light. This is illustrated in Fig. 5 which displays the charge distribution Q obtained at U_{acc} = 25 kV. The mean number of electrons Ne per bunch which defines the deposited energy is determined from the relation,

$$N_e = ENF\left(\langle Q \rangle / \sigma_Q\right)^2 \qquad (1)$$

with <Q> and σ_Q being the mean value of the charge distribution and its variance, respectively. *ENF* is the Excess Noise Factor of the PMT (*ENF* ~ 1.1 was derived from the peak-to-valley ratio of this PMT for single photons). The mean deposited energy per bunch is,

$$E_d = e \cdot N_e \cdot U_{acc} \qquad (2)$$

The analysis of the data shown in Fig. 5 leads to a mean number of electrons in the bunch of N_e = 10.

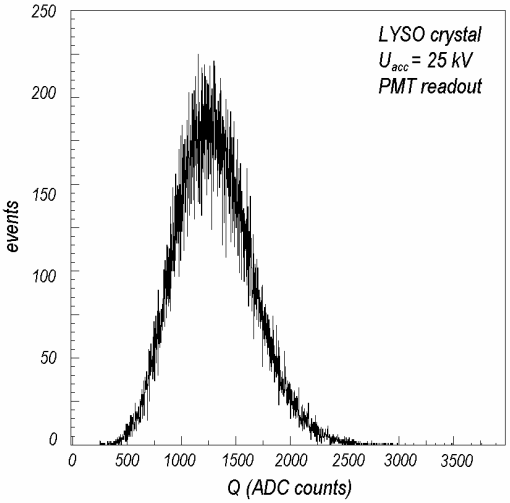

Fig. 5: Example of a charge spectrum before pedestal subtraction (1 ADC count = 50 fC). The LYSO crystal bars were bombarded with bunches of on average 10 electrons. The acceleration voltage was set to 25 kV. The mean and RMS value of the distribution are 1305 and 350.5 ADC counts, respectively.

However, the deposited energy, which is finally converted to scintillation light is reduced by two well known low energy effects: (1) a fraction (~45 %) of the electrons is back scattered from the crystals without depositing their full energy [3], (2) the light yield of the LYSO crystal at low energies (up to ~100 keV) is not linear with the deposited energy. The

latter effect is described by the so-called Relative Light Output (*RLO*). For LSO crystals *RLO* values of 0.8 have been measured for an energy deposition of 25 keV [4]. They approach 1 for depositions above 50 keV.

We take into account both effects by introducing a parameter κ which depends on the acceleration voltage U_{acc}. An electron bunch of energy $e \cdot N_e \cdot U_{acc}$ hitting the crystal leads to an amount of energy E_c which is actually converted to scintillation photons

$$E_c = e \cdot N_e \cdot U_{acc} \cdot \kappa(U_{acc}) \qquad (3)$$

We can extract $\kappa(U_{acc})$ for LYSO in a linear approximation directly from our measurements.

IV. Experimental Results

The main objectives of this study are

1. the experimental proof that the light output of the WLS strips is sufficient to observe the light created not only by the absorption of 511 keV gamma rays but also by Compton recoil electrons in the LYSO crystals down to ~ 50 to 100 keV;
2. the measurement of the resolution of the digital z-coordinate reconstruction.

A. Photoelectron yield of the LYSO crystal bars

In Fig. 6, left hand side, the photoelectron yield is plotted versus the converted energy *Ec*, calculated according to eq. 3. The parameter $k(U_{acc})$ has been determined in two different ways: (1) from the MC (using measured Relative Light Output data for LSO), and (2) by fitting κ in a linear approximation $\kappa(U_{acc}) = a + b \cdot U_{acc}$ such that the photoelectron yield can be described as $Npe = c \cdot E_c$. The fit leads to $\kappa(U_{acc}) = 0.501 + 0.0117 \cdot U_{acc}$. The two methods to determine κ differ on average by only 4%. Extrapolation of the photoelectric yield to 511 keV results in 1050 ± 20 photoelectrons.

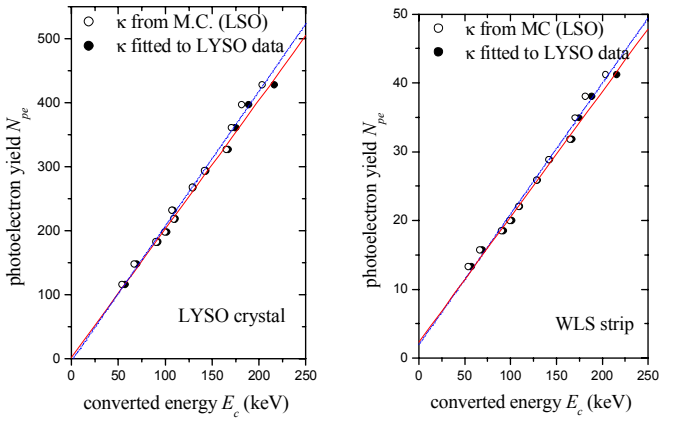

Fig. 6: Readout of the LYSO bars (left) and WLS strips (right hand side). The plots show the dependence of the number of detected photoelectrons on the converted energy.

Under the assumption of an intrinsic LYSO energy resolution of 7 % (FWHM), a photoelectron yield of 1050 at 511 keV is expected to lead to an energy resolution of ~11 % (FWHM), in agreement with our previous measurement [2].

B. Photoelectron yield of the WLS – strip readout

The gain of the MPPCs was adjusted to $4 \cdot 10^5$ providing a total gain of the readout chain of $12 \cdot 10^6$ including the gain of the serial fast amplifier.

In Fig. 6, right hand side, shows the sum of the number of detected photoelectrons in the two WLS strips as a function of the converted energy. As for the LYSO bars, the photoelectron yield in the strips varies linearly with the converted energy. At E_c = 200 keV a yield of is 39 ± 2 is measured, which extrapolates to about 100 photoelectrons for 511 keV gamma rays. Correcting for the optical cross talk of the MPPCs (~ 20 %), the effective number of detected photons from the WLS strips is estimated to be about 80. This result is expected to ensure high detection efficiency also for the reconstruction of Compton recoil electrons in the energy range of 50 to 100 keV.

Fig. 7 shows the profiles of the number of detected photoelectrons in a scan of the light spot transverse to the WLS-strips, i.e. along the LYSO crystals. The data were obtained at U_{acc} = 25 kV for a mean converted energy of E_c = 200 ± 12 keV.

Fig. 7 (left) shows the profile of the number of detected photoelectrons for each strip and Fig. 7 (right) the sum of both strips. The width covered by the strips (approximately -3 < z_{mir}< 3 mm) is indicated on the figures.

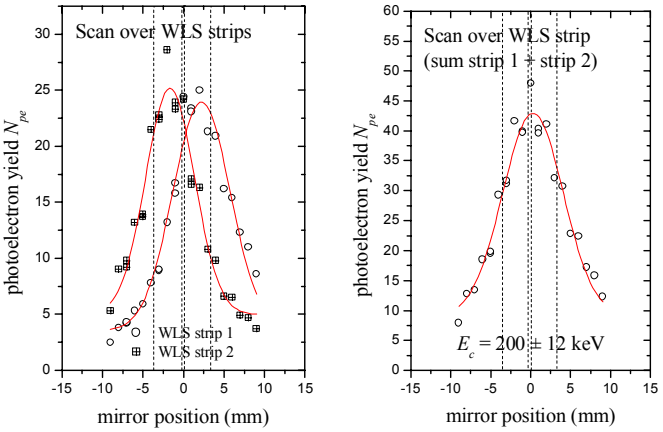

Fig. 7: Photoelectric yield during the scan over the WLS strips. Left hand side: Yield of the individual strips. Right: Sum of the strips. The dashed vertical lines indicate the approximate position of the strips.

C. Determination of the axial z coordinate and precision of the reconstruction.

To perform the reconstruction several selected discrimination thresholds were applied by software to the charge read out from the strips. If a signal is detected from both strips the reconstructed z coordinate is assumed in between the two strips (z_{rec} = 0). Otherwise, if only one of the strips has a signal, the z coordinate is reconstructed in the centre of the hit strip (z_{rec}= -1.5 or +1.5 mm).

For a given z_{mir} position of the mirror, the z_{rec} coordinate in Fig. 8 is determined from the mean value of the experimental distribution, and the resolution from the RMS value of the distribution. The measured RMS values are in the range of 0.7 to 0.9 mm in good agreement with M.C simulations

Fig. 8 shows the reconstructions obtained for a scan orthogonal to the strips at a mean energy E_c = 310 ± 32 keV and a set of discrimination thresholds equivalent to 5, 10, 15 and 20 photoelectrons, respectively.

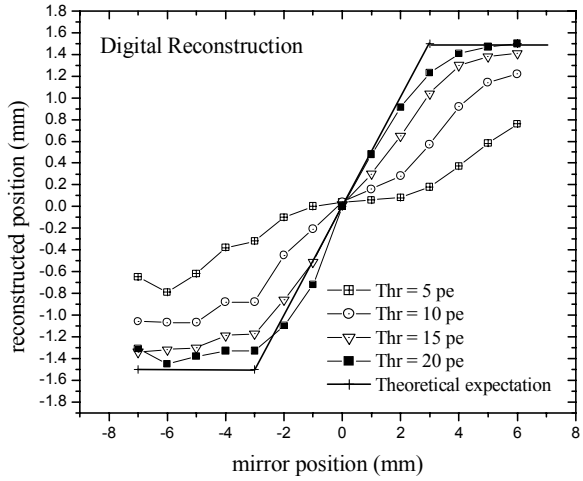

Fig. 8: Scan of the light spot over the two WLS strips at an energy E_c = 310 keV converted in the LYSO crystal.

The deviations with respect to the expected reconstruction shown on the figure, especially outside the interval covered by the strips (-3 $< z_{mir} <$ 3 mm), are dependent on the discrimination threshold. Since both strips are more frequently hit when decreasing the discrimination threshold, the mean value of the distributions is consequently forced towards z_{rec}= 0. This is an artificial bias due to the limitation to two strips only and will not be present in a module with more strips. The four curves in Fig.8 also suggest that the discrimination threshold should be chosen proportional to the energy deposited in the LYSO bars in order to improve the resolution in particular for the reconstruction of Compton interactions.

D. Photoelectric yield and energy resolution of a LYSO crystal bar with MPPC readout

In a modified set-up a LYSO crystal bar was read out at one end with a MPPC. Standard optical grease was used at the interface. The opposite end was not read, but as before left with its reflective Aluminium coating. The energy range of the electron source was increased such that a range from E_c = 66 to 534 keV could be measured. The number of detected photoelectrons was again derived from the ADC spectrum. The data is shown in Fig. 9. The Polynomial fit (2nd order) to the data predicts for E_c = 511 keV a photoelectron yield of N_{pe} = 1317. Above N_{pe} = 600 the non-linearity of the MPPC due to the limited number of cells (N_{cell} = 3600) becomes apparent. The data can be corrected for this combinatorial saturation effect and can then in good approximation be described by a linear fit.

The expected energy resolution, which is also shown in Fig. 9, has been derived from the data using the formula

$$\Delta E / E \ \ (\mathrm{FWHM}) = 2.35 / \sqrt{N^*_{pe}} \oplus (\Delta E/E)_{\mathrm{intr.}} \qquad (4)$$

The quantity N^*_{pe} is the number of detected photoelectrons after subtracting 20% cross-talk. The intrinsic resolution of LYSO $\Delta E/E_{intr}$. is 7% [5]. The expected resolution at E_c = 511 keV is close to 10% (FWHM).

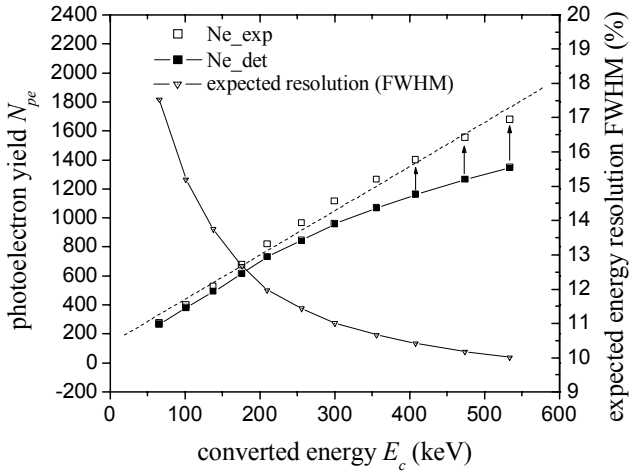

Fig. 9: LYSO bar with MPPC readout. The plot shows the number of detected photoelectrons, as measured, and after a correction for the occupancy of the micro-pixels of the MPPC. The latter are described in good approximation by a straight line fit. The expected energy resolution is derived directly from the measured N_{pe}.

V. Conclusions and Next Steps

The results obtained with the test setup, consisting of two LYSO crystals and two WLS strips readout by Hamamatsu MPPCs, type S 10362-33-050C, show that a full 3 D readout of PET modules with the axial concept is feasible. The light yield at an equivalent energy of 511 keV, deposited with a low energy electron beam in the LYSO crystal, was determined by extrapolation to be 80 p.e.. This yield is sufficient to measure the axial coordinate of ~50 keV to 350 keV Compton recoil electrons with good precision. The axial spatial resolution measured in the test set-up was determined to be 1.9 mm FWHM at 511 keV for digital coordinate reconstruction. These values can be improved in a bigger setup with many LYSO crystals and WLS strip arrays.

We are at present building two modules of 36 LYSO crystals ($3 \times 3 \times 100$ mm^3) each with about 200 WLS strips placed in the gaps of the LYSO stack (3.4 mm pitch). Both LYSO bars and WLS strips will be read out with tailor-made G-APD devices of dimensions 3.2×3.2 mm^2 and 3×1.2 mm^2, respectively (SiPM developments are pursued in collaboration with Hamamatsu and IRST). The signals from the SiPMs will be fed to the inputs of the self-triggering VATAGP-5 chip, which was developed and fully tested for the AXIAL HPD PET project [6]. The readout of SiPMs from IRST and Hamamatsu, using one channel of a VATAGP-5 chip has already been demonstrated. One layer of a demonstrator module is shown in Fig. 10. The implementation of the two modules will enable us in the near future to assemble a demonstrator set-up for a full study of sensitivity and spatial and energy resolution of an axial 3-D PET.

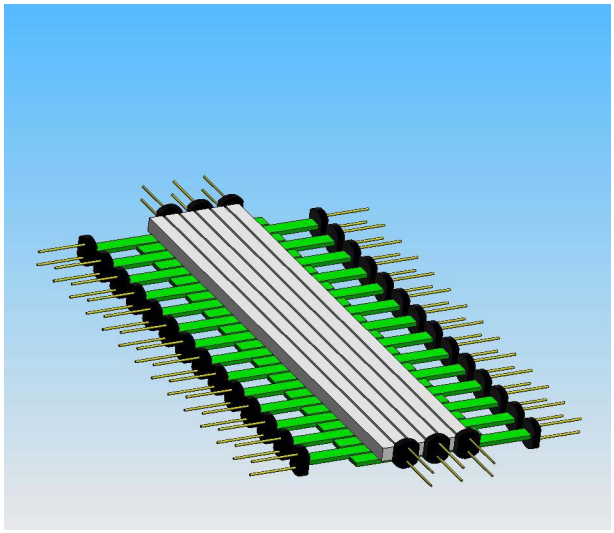

Fig. 10: One Layer of a demonstrator module consisting of 6 LYSO crystals of 3 mm x 3 mm x 100 mm and 28 WLS strips readout on opposite sides by tailor made SiPM devices.

ACKNOWLEDGMENT

We would like to thank our technical staff, C. David, A. Folley, M. van Stenis (CERN), L. Dell'Olio and G. De Carne (INFN Bari) for their excellent work in the preparation of the mechanical and optical components used in the tests.

REFERENCES

[1] J. Séguinot et al., Il Nuovo Cimento C, Volume 29 Issue 04 (2005) p429.
[2] A. Braem et al., Nucl. Instr. Meth. A 580 (2007) p1513.
[3] E.H. Darlington, J. Phys. D, Vol. 8, (1975) p85.
[4] W.W. Moses, Nucl. Instr. Meth. **A** 487 (2002) p123.
[5] C. M. Pepin et al., IEEE Trans. Nucl. Science, Vol. 51, No. 3 (2004) p789.
[6] A. Braem et al., Nucl. Instr. Meth. **A** 5 71(2007) p134.